

# Generation of High Resolution DSM Using UAV Images

Biplov BHANDARI, Upendra OLI, Uttam PUDASAINI, Niroj PANTA, Nepal

**Keywords:** GNSS/GPS, Photogrammetry, UAV, DSM, Digital Image Processing, 3D

## SUMMARY

Generating High Resolution DSM often demands highly accurate data. Among the range of terrestrial and aerial methods available to produce such a dataset, this project tests the utility of images acquired by a fixed wing, low cost Unmanned Aerial Vehicle (UAV). The data processing of UAV images have been carried out using the algorithms ranging from classical photogrammetry to modern Computer Vision (CV) algorithms.

Nowadays, the use of UAV has increased to offer fast, easy and cost effective way to capture high resolution images for a comparatively smaller area. In this paper, we present a state-of-the-art photogrammetry and image processing techniques provided by different software and their algorithms. The key element in a UAV photogrammetric data processing of the images which have been obtained with large variation in its geometry is the accurate georeferencing.

27 high resolution (2.4 cm average spatial resolution) UAV-acquired images of a sand mine at Tielt-Winge, Belgium has been used for this project. All the images have been acquired by a Sony Nex-5R digital camera mounted on a Trimble UX5 Imaging Rover, a fixed wing UAV. Although three software: LPS, AgiSoft PhotoScan and PIX4D were used for image processing. The identified algorithms and limitations in processing are valid for most other commercial photogrammetric software available on the market.

The effort and the achievable accuracy of DSM result from every process are compared using the highly accurate ground control points as the reference data. The comparison of the DSM is performed through difference of DSM, RMSE and visual interpretation and to conclude SIFT algorithm and Dense Stereo matching provide good result for UAV data compared to traditional digital image matching using Forstner interest operator and ultimately provided centimeter level accuracy in the output results. However for certain areas like forest and vegetation, poor results were obtained due to poor image matching.

# Generation of High Resolution DSM Using UAV Images

**Biplov BHANDARI, Upendra OLI, Uttam PUDASAINI, Niroj PANTA, Nepal**

## 1. INTRODUCTION

Generally speaking, DSM is the 3D representation of the terrain of the earth surface along with other man-made and natural objects over it. Highly-accurate and high-resolution DSMs are useful in a variety of works ranging from general construction survey to viewpoint selection, line of sight analysis, urban planning, flood modeling and simulation and many other works where data related to elevation of earth surface is of greater importance [1]. This requires accurately measured points with 3D coordinates. There are different techniques for obtaining mass points for DSM generation like Photogrammetry, Satellite Remote Sensing, terrestrial surveying etc. In the project, the photogrammetric method for generation of DSM from high resolution images acquired by a digital camera mounted on a fixed wing UAV has been used.

Unmanned aerial vehicle (UAV) generally refers to uninhabited flying vehicle that fly based on the pre-entered program or on its own recognition of the surroundings [4]. They can be remotely controlled, either semi-autonomous, autonomous, or have a combination of these capabilities. Various types of payloads can be fitted thereby making them capable of performing specific tasks within the earth's atmosphere, or beyond, for a certain duration related to their specific tasks [5].

The limited payload makes it unable to use professional aerial photogrammetric hardware like calibrated aerial camera and the UAV is also affected by the wind because of its low weight [6]. As a result the images acquired by this process have a relatively higher amount of distortions. Thus the processing of UAV images to obtain accurate high resolution products are rarely supported by classical photogrammetric workflows. New algorithms and techniques from Computer Vision makes it possible to generate comparatively better outputs [4].

In the recent time, UAV acquired images are being widely used for high resolution digital surface modelling, reconstruction and monitoring of glacier, Large Scale Mapping, forest-fire monitoring, disaster management, mapping urban and suburban areas, environmental and natural resources monitoring and many more.

The main focus of this project is a comparative study where software from classical photogrammetry as well as computer vision are used for the photogrammetric data processing for the ultimate purpose of DSM Generation.

The main objective of the study is to create a Digital Surface Model (DSM) using high resolution images acquired by a digital camera mounted in a UAV platform. Following are the sub objectives developed to achieve the main objective.

- To orient and georeference UAV images using interior and exterior orientation parameters.
- To generate high resolution DSM.
- To compare and analyze the accuracy of DSM generated from different methods.

## **2. METHODOLOGY**

### **2.1 Comparison between Aerial and UAV Photogrammetry**

UAVs still haven't been well established as a standard platform for conducting activities related to photogrammetric measurements [6]. There are several such factors that makes the photogrammetric applications complex using this system. A comparison of such factors with standard aerial photogrammetry is essential for understanding the complexities associated with this technology and move accordingly during image processing. Table 1 compares the low cost UAV's carrying normal consumer grade cameras with the aerial photogrammetry.

Table 1: Comparison between Aerial and UAV Photogrammetry

| <b>Particulars</b>        | <b>Aerial Photogrammetry</b>   | <b>UAV Photogrammetry</b>                           |
|---------------------------|--|---|
| Data Acquisition          | Manual/Assisted  | Assisted/Manual/ Automatic                          |
| Aerial Vehicle            | Highly stable specially designed aircrafts                                   | Small aerial Vehicles with certain payload capacity |
| GPS/INS Configurations    | cm-dm  | cm-10 m   |
| Image Resolution          | cm-m   | mm-m  |
| Ground Coverage           | Km <sup>2</sup>  | M <sup>2</sup> -km <sup>2</sup>                     |
| Cameras                   | Well calibrated cameras especially designed for photogrammetric applications | Can work with normal off-shelf digital cameras      |
| Fiducial Marks            | Present  | Absent  |
| Flying Height             | 100 m-10 km  | m-km<br>(not more than 1 km)                        |
| Data Processing Workflows | Standard Photogrammetric Workflow  | No standard workflows                               |
| Salient Feature           | Better control over the output image quality                                 | High temporal accuracy with real time applications  |

## 2.2 Project Site

A sand mine located at Tielt-Winge, Belgium ( $2^{\circ}30'E$  to  $6^{\circ}30'E$  and  $49^{\circ}30' N$  to  $51^{\circ}30' N$ ) has been selected as the project site. The total area covered by this mine is around 0.0395 sq.km. The average terrain height according to the GCP configuration throughout the area is around 134.1718 m. This project uses 27 images from four different flight strips.

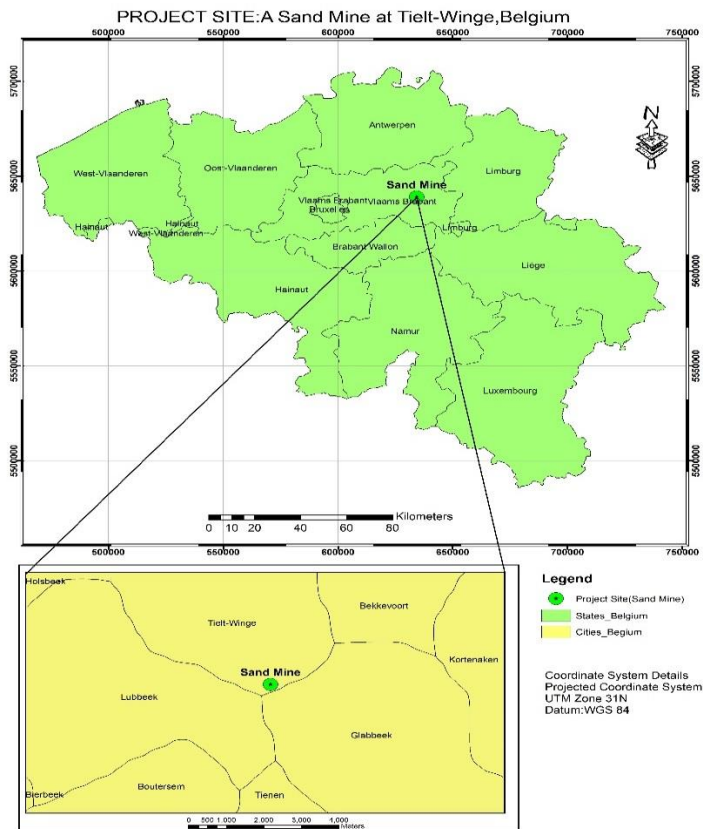


Figure 1: Project Site: A sand mine at Tielt-Winge, Belgium

## 2.3 Materials Used

### 2.3.1 Data

All the data for this project have been provided by the popular software company Trimble<sup>1</sup>. The images have been acquired by Trimble UX5 Aerial Imaging System<sup>2</sup>, a fixed wing UAV which have been developed by Trimble Company. A total of 41 images were taken by the Sony Nex-5R digital camera to model an area of 0.042 sq. km.

Table 2: Collected Data and Details

| SN | Particulars                  |                         | Details          |                    |
|----|------------------------------|-------------------------|------------------|--------------------|
| 1  | GSD                          |                         | 2.4 cm           |                    |
| 2  | Pixel Size                   | X-Direction             | 4.75 $\mu$       |                    |
|    |                              | Y-Direction             | 4.75 $\mu$       |                    |
| 3  | Average along Image Overlap  |                         | 60%              |                    |
|    | Average across Image Overlap |                         | 80%              |                    |
| 4  | Image Size                   |                         | 4912*3264 pixels |                    |
| 5  | Camera Calibration           | Focal Length            |                  | 15.5172 mm         |
|    |                              | Principal Point         |                  | 0,0                |
|    |                              | Radial lens distortions | K1               | -0.00020291        |
|    |                              |                         | K2               | 0.000000681845     |
|    |                              |                         | K3               | -0.000000000864898 |

<sup>1</sup> <http://www.trimble.com/>

<sup>2</sup> <http://www.trimble.com/Survey/ux5.aspx>

|   |                       |                            |  |               |
|---|-----------------------|----------------------------|--|---------------|
|   | Parameters            | Tangential Lens Distortion | T1   | -0.0000296516 |
|   |                       |                            | T2   | 0.000050424   |
| 6 | Ground Control Points | Parameters                 | 13 GCP's with S.D in x,y=2 cm and S.D in z=3 cm<br><br>Images showing the ground location of GCP |               |
|   |                       | Coordinate System Details  | Projected Coordinate System, UTM Zone 31 North<br><br>Vertical Datum = MSL                       |               |
| 7 | GPS/INS Data          | Parameters                 | X,Y,Z location of camera centers with rotational parameters (omega, phi and kappa)               |               |
|   |                       | Coordinate System Details  | Projected Coordinate System, UTM Zone 31 North<br><br>Vertical Datum =W.G.S 84                   |               |

### 2.3.2 Software

**i. LPS:** LPS, a photogrammetric package i.e. found integrated with ERDAS Imagine software is initially developed for processing of aerial images. LPS provides tools for manual and automated tie point measurement and aerial triangulation so as to process and analyze the airborne imagery.

**ii. AgiSoft PhotoScan:** AgiSoft PhotoScan, based on the latest multi-view 3D reconstruction technology, operates with arbitrary images and is efficient in both controlled and uncontrolled conditions. Both image alignment and 3D model reconstruction are fully automated in this software. AgiSoft PhotoScan (version 1.0.4) is used in this project because of its massive and successful usage for 3D modeling.

**iii. PIX4D:** PIX4D is a popular commercial software package developed by PIX4D Company. The salient feature of this software is that it allows optimization in the processing results by introducing ray cloud editor, an interactive 3D point clouds editing interface where users can edit the 3D point clouds and enhance the accuracy of their project<sup>3</sup>.

**iv. ArcGIS:** ArcGIS is a popular software package by ESRI for working with maps and geographic information. Arc Map version 10 was used for the purpose of accuracy assessment of output DSM's. Also all the activities related with map preparation were performed using this software.

---

<sup>3</sup> <http://pix4d.com/raycloud/>

## 2.4 Data Preparation

Generation of DSM from images requires a consistent data. For this project two major changes were done to achieve consistency in the coordinate system of obtained data. Firstly, transformation was done to convert the horizontal coordinate system (WGS 84) of camera location into projected coordinate system (WGS 84, UTM Zone 31N). Then, elevation difference was calculated in order to bring consistency in reference system for the elevation of provided datasets. Figure 2 shows the location of place marks which were used to find the elevation difference between the ellipsoid and geoid using a web based application, GeoidEval<sup>4</sup>.



Figure 2: Location of 10 different Place marks (PM1 to PM10) used to estimate the elevation difference between reference datum.

## 2.5 Photogrammetric Data Processing

Two different methods have been adopted for the purpose of georeferencing as well as generating DSM from UAV images. The first one is the use of classical photogrammetric workflow and the second one is the use techniques from computer vision (CV). The methodologies followed by both of them are shown in figure 3 and figure 4 respectively.

---

<sup>4</sup> <http://geographiclib.sourceforge.net/cgi-bin/GeoidEval>

### Photogrammetric data processing using Classical photogrammetric approach

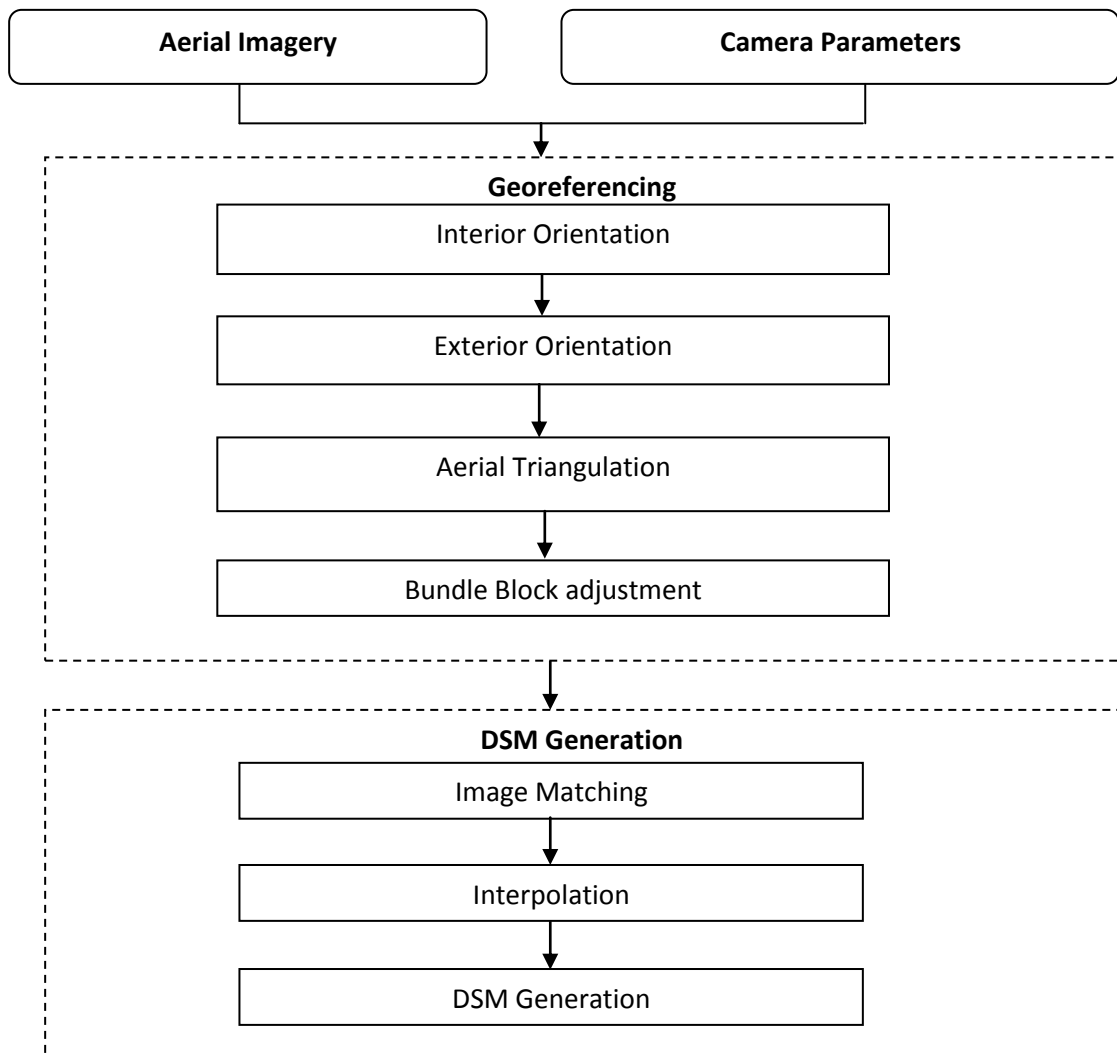


Figure 3: General Photogrammetric process for generating DSM from UAV images

## Photogrammetric data processing using Computer Vision

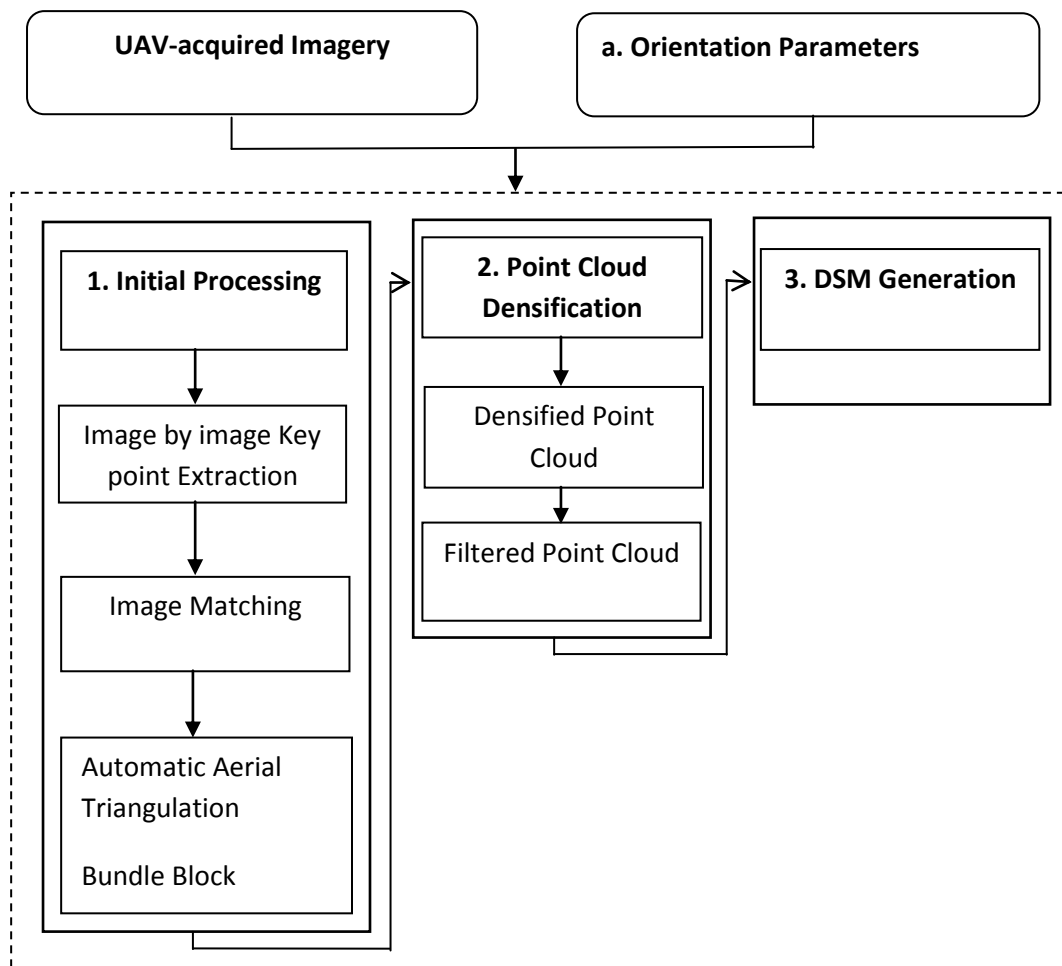


Figure 4: General workflow for modern computer vision techniques

The brief descriptions of these individual approaches have been made by categorizing all of the intermediate steps into two major steps georeferencing and DSM generation. Following is the description of these individual steps.

## 2.5.1 Georeferencing of UAV Images

### 2.5.1.1 Georeferencing using Classical photogrammetric approach

Leica Photogrammetric Suite, henceforth described as LPS uses classical photogrammetric approach for georeferencing UAV images. First of all a new block file is created in LPS. Followed by providing information about camera model where various information like coordinate system, interior orientation parameter, flying height, principal point and distortion parameters (radial and tangential) are defined. The exterior orientation parameters,  $X_0$ ,  $Y_0$ ,  $Z_0$ ,  $\omega$ ,  $\phi$  and  $\kappa$ , can be provided at the time of project set-up or later after performing interior orientation. Tie point generation and bundle block adjustment marks the completion of exterior orientation in LPS. The process of tie point generation in LPS makes use of Forstner interest operator [10] [11]. LPS provides two modes for tie point generation: manual and automatic. As manual tie point generation would be time-consuming although being accurate, we adapted automatic tie point generation. For tie point generation, various strategy can be defined where we can change the size of search window, correlation window size, least square window size, correlation coefficient and many others [2].

The next step after tie point generation is to find the corresponding match for that feature point. The image matching strategies in LPS include the coarse-to-fine; feature-based matching with geometrical and topological constraints, which is simplified from the structural matching algorithm [7]; and the least square matching for the high accuracy of tie points. The precision of cross-correlation is limited to one pixel. With Least square optimization, the precision is increased up-to  $1/10^{\text{th}}$  of a pixel.

The next step is the computation of 3D coordinates of the matched points through Aerial triangulation. The statistical weight related to GCP measurement, exterior and interior orientation parameters can be assigned accordingly.

Moreover LPS also offers the use of different models to optimize the result of aerial triangulation through Bundle Block Adjustment (BBA). It includes different model like model like Bauer's simple model, Jacobsen's simple model, Ebner's orthogonal model and Brown's physical model, Lens Distortion Model [8] for improving the results. Lens Distortion Model [3] can be used in cases where digital cameras with known calibration parameters is being used.

### 2.5.1.2 Georeferencing using Computer Vision Science

Two commercial software packages: AgiSoft PhotoScan and PIX4D using algorithms from computer vision have been used for georeferencing the images.

The data processing begins with the project set up where the images, camera calibration parameters and the exterior orientation parameters are entered into the respective software.

Image by image key point extraction occurs in the next phase. Both of these software use SIFT algorithm [12][13] for extraction of accurate key points in individual images. The individual software have optimized the SIFT algorithm so as to provide better results.

The use of Ground Control Points helps to accurately georeference the point clouds generated after accurate image matching. These software provides a semiautomatic way for entering the ground control point data.

Automatic aerial triangulation [14] helps to compute the 3D coordinates of individual key points. The GPS/INS information which was entered during the project setup provides the absolute reference to the image block with a rough accuracy of GPS system (few meters). Accurate ground control data are used to optimize the parameters with higher accuracy.

Entire image block is now adjusted using the bundle block adjustment technique so that accurate information related to position and orientation of camera for every image is recomputed. In case AgiSoft PhotoScan, it finds approximate camera locations using a greedy algorithm based on the input orientation parameters and refines them later during bundle-adjustment technique while in case of PIX4D the automatic AT and BBA helps in optimization of all image parameters with relatively high accuracy<sup>5</sup>.

### 2.5.2 DSM Generation

#### 2.5.2.1 DSM Generation using Classical Photogrammetric approach

DSM generation using classical photogrammetric approach is an automatic process in LPS which consists of three major steps. The first step is Image Matching step where all of the input images are matched and stitched together in order to form a single mosaic image using

---

<sup>5</sup> <http://www.pix4d.com>

digital image matching technique [15].LPS performs this through automatic tie point generation and BBA.

The second step is the generation of dense 3D cloud points. LPS generates the 3D point cloud while performing tie points, whose 3D coordinates are calculated at the time of Bundle Block Adjustment. The final step is to build a 3D model around the point cloud. We generated DSM in LPS through Automatic Terrain Extractor (ATE).

LPS ATE is mainly used for fast, automatic and accurate terrain extraction with built-in accuracy. It is generally intended for very rapid terrain production at a relatively lower point cloud density than eATE<sup>6</sup>. It offers correlation strategies, output settings, and classification options. DSM of cell size 0.025 m was produced using the ground control points and check points of block to control the error in DSM.

The output for DSM in LPS can be either a mosaicked DSM or individual DSM for individual image pairs.

#### 2.5.2.2 DSM Generation using Computer Vision Science

The sparse point clouds generated during the initial processing step consists only of key points that were successfully matched and verified along the multiple images. In fact there are potentially many more matches that results to a much more dense point clouds. This step is also fully automated step in both the software: AgiSoft PhotoScan and PIX4D. A dense stereo matching algorithm [16] is used to generate dense point clouds. Millions of points with known ground coordinates are generated during this phase. These generated dense point cloud may contain gaps well known as holes at those locations where the image matching has failed. Such locations can be edited by editing the point clouds. In this regard both of these software allows the 3D editing through an interactive interface.

The dense point clouds generated this way are then interpolated to form a triangulated irregular network in order to obtain a digital surface model. After generating mesh, DSM can be exported in different formats such as Arc/Info Elevation Data (\*.asc), BIL (\*.bil), XYZ (\*.xyz) and GeoTIFF Elevation Data (\*.tif).

---

<sup>6</sup> <http://www.hexagongeospatial.com/products/imagine-photogrammetry/LPSeATE/Details.aspx>

## 2.6 Accuracy Assessment of DSM

The best method to assess the accuracy of a DSM is to compare the elevation of DSM at certain locations which are well spread throughout the area. For this purpose accurately measured ground control points need to be taken as reference points. This project made use of ArcGIS software for accuracy assessment where five ground control points 2003, 2004, 2006, 2007, and 2010 were used as the reference data during comparison with elevation of same locations from the DSM. The comparison of DSM from different software becomes consistent only if all the DSM's are in the same file format and of same spatial resolution. In our case all the DSM's were in a .tif file format and have a spatial resolution of 2.5 cm. Finally accuracy of individual DSM was calculated in the form of RMSE<sup>7</sup>. A set of check points used for accuracy assessment of DSM aren't well distributed. Thus visual interpretation and analysis was carried out to explain the possible causes behind the errors at certain locations. Moreover, Difference of Surfaces [9] was also calculated so that it helps to compare how much difference exists between the output DSM's of same area generated by different approaches.

---

<sup>7</sup> <http://statweb.stanford.edu/~susan/courses/s60/split/node60.html>

### 3. RESULTS AND DISCUSSIONS

#### 3.1 Image Matching

The classical photogrammetric application like LPS that makes use of Forstner interest operator allows customization of different parameters for tie point's generation and image matching successively. Different parameters as mentioned in table 3 were varied and the matching success was checked to determine a final result.

Table 3: Results of variation in the strategy parameters during tie point generation using LPS

| Parameters  | Matching Success | Total Number of Tie Points |
|---|------------------|----------------------------|
| Initial Accuracy = 0.005%<br>Correlation Coefficient = 0.80<br>Window search size = 10<br>Point per Image = 500 | 32.69 %          | 234                        |
| Initial Accuracy = 25%<br>Correlation Coefficient = 0.80<br>Window search size = 15<br>Point per Image = 200    | 86.35 %          | 1128                       |

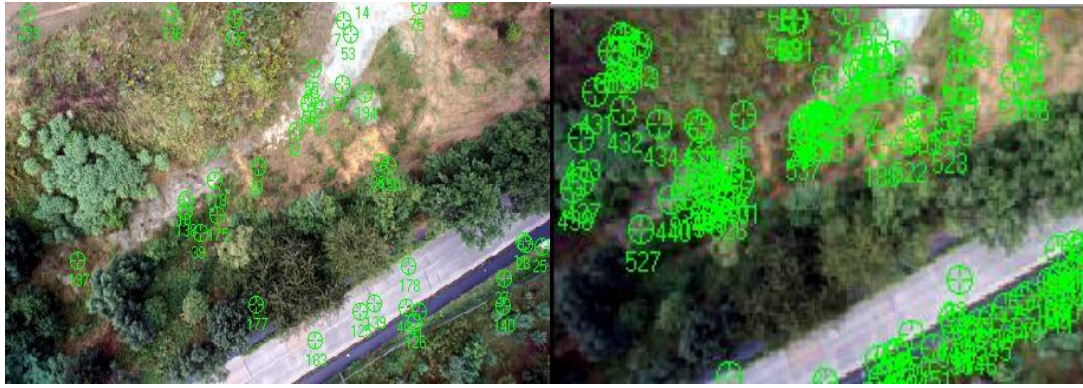


Figure 5: Images showing the distribution of tie points in an image as a result of variation in parameters as shown in table 3

### 3.2 Georeferencing

Georeferencing is another major issue in DSM generation because images need to be accurately georeferenced for a good representation of ground reality. We used different software for this purpose. Out of the thirteen control points measured with an accuracy of 2 cm in X, Y and 3 cm in Z direction, 8 control points were used for this purpose. Five of these control points were used during bundle block adjustment while 3 control points were used as check points for independent check of the output.

Table 4: Error information associated with check points during georeferencing using LPS

| <b>Point No</b> | <b>Error in X<br/>(cm)</b> | <b>Error in Y<br/>(cm)</b> | <b>Error in Z<br/>(cm)</b> | <b>Type</b>  |
|-----------------|----------------------------|----------------------------|----------------------------|--------------|
| 2008            | 1.94                       | -7.69                      | 0.85                       | Check Points |
| 2005            | -11.91                     | 9.03                       | 4.81                       | Check Points |
| 2012            | 27.38                      | 9.47                       | 6.02                       | Check Points |
| <b>RMSE</b>     | 17.27                      | 8.76                       | 4.47                       |              |

Table 5: Error information associated with check points during georeferencing using AgiSoft

| <b>Point No</b> | <b>Error in X<br/>(cm)</b> | <b>Error in Y<br/>(cm)</b> | <b>Error in Z<br/>(cm)</b> | <b>Type</b>  |
|-----------------|----------------------------|----------------------------|----------------------------|--------------|
| 2008            | 3.63                       | -2.02                      | -6.03                      | Check Points |
| 2005            | 0.44                       | -0.27                      | -0.93                      | Check Points |
| 2012            | -0.58                      | 0.46                       | 5.80                       | Check Points |
| <b>RMSE</b>     | 2.13                       | 1.21                       | 4.86                       |              |

Table 6: Error information associated with check points during georeferencing using PIX4D

| <b>Point No</b> | <b>Error in X<br/>(cm)</b> | <b>Error in Y<br/>(cm)</b> | <b>Error in Z<br/>(cm)</b> | <b>Type</b>  |
|-----------------|----------------------------|----------------------------|----------------------------|--------------|
| 2008            | -2.23                      | 1.72                       | 0.81                       | Check Points |
| 2005            | -0.85                      | -2.21                      | -2.95                      | Check Points |
| 2012            | 0.42                       | -3.24                      | 4.17                       | Check Points |
| <b>RMSE</b>     | 1.4                        | 2.47                       | 2.98                       |              |

From tables 4, 5 and 6 shows that the results of georeferencing is much better in case of AgiSoft and PIX4D. It is because the algorithms involved are able to automatically locate the ground control in all other images provided that the user locate a control point in any one or two images initially. AgiSoft uses guided marker placement approach<sup>8</sup> such that locating control points on at least one image is sufficient to have an approximate location of points on all other images. In case of PIX4D the control points should be located on at least two images in order to determine its position on other images. Moreover PIX4D also allows to insert the ground coordinates in the 3D point cloud editing window which makes the georeferencing work more accurate. Thus better accuracy is obtained in case of georeferencing from software

---

<sup>8</sup> <http://www.agisoft.ru/tutorials/photoscan/>

based on modern computer vision. However in case of LPS, the control points should be manually uploaded in every single image. This manual approach increased the chance of having more error in georeferencing since a user can't always accurately mark on the same pixel at all images.

### 3.3 DSM Generation:

The DSM's generated from individual software are shown in Figure 6, 7 and 8 respectively.

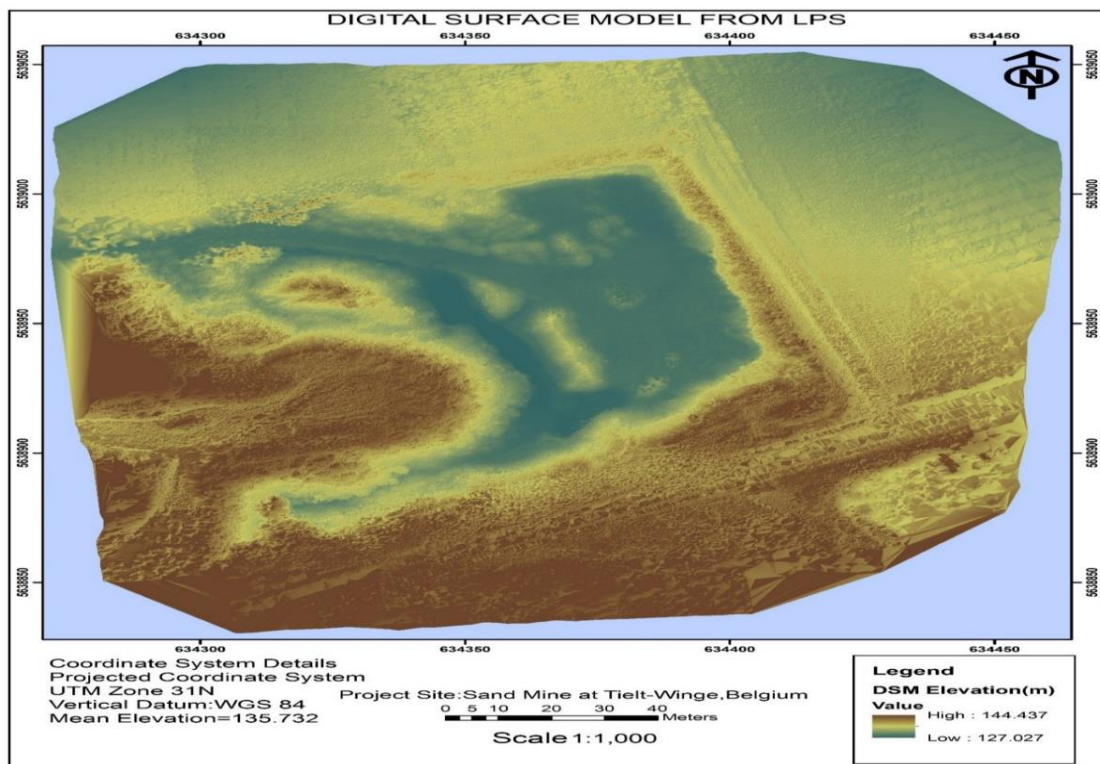


Figure 6: DSM generated from LPS

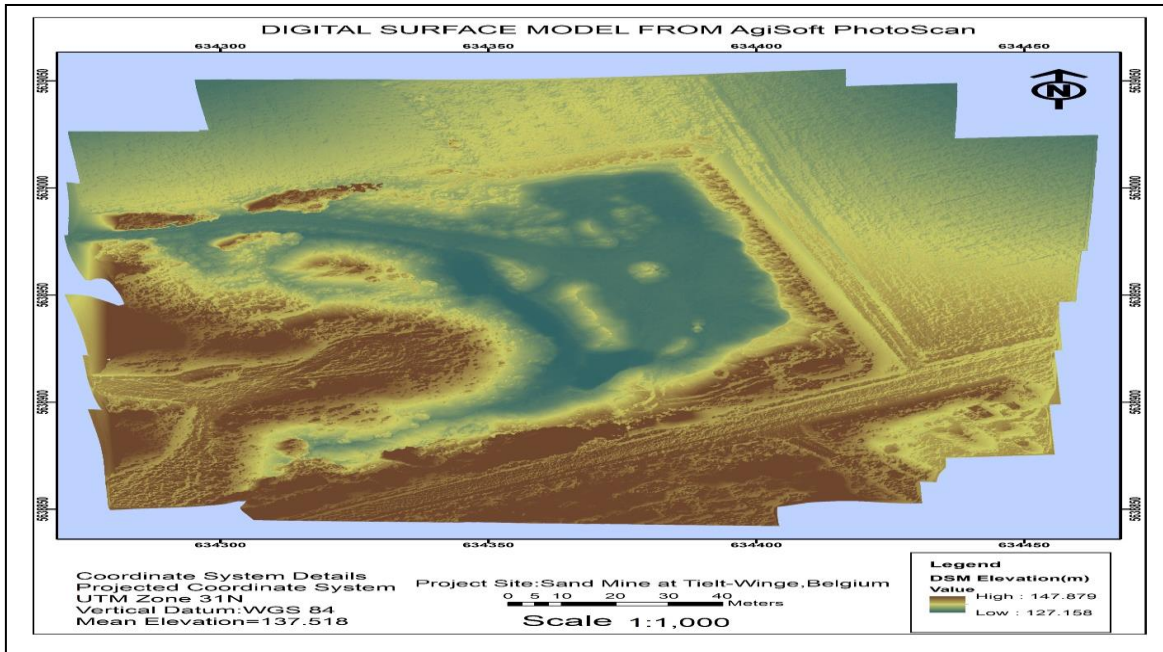


Figure 7: DSM generated from AgiSoft PhotoScan

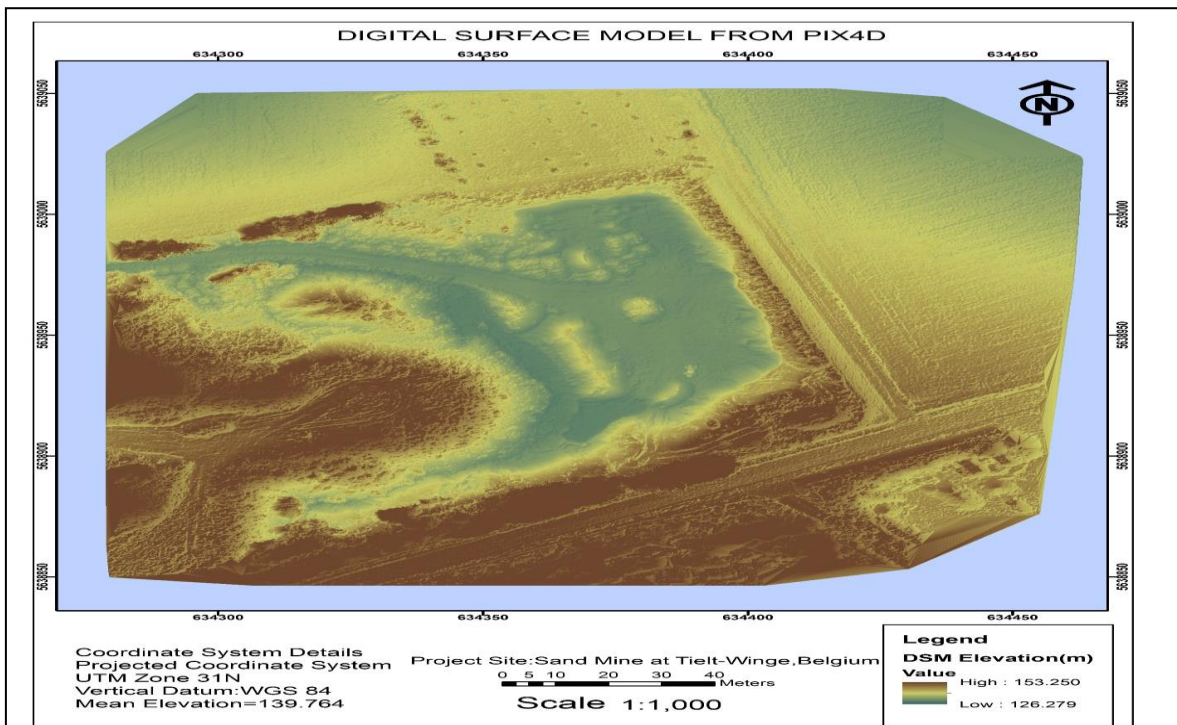


Figure 8: DSM Generated from PIX4D

Generation of High Resolution DSM Using UAV Images (7439)  
 Biplov Bhandari, Upendra Oli, Niroz Panta and Uttam Pudasaini (Nepal)

FIG Working Week 2015  
 From the Wisdom of the Ages to the Challenges of the Modern World  
 Sofia, Bulgaria, 17-21 May 2015

Two of the major parameters: spatial extent and the elevation range of the DSM's seem to be different for outputs from different processes. In case of LPS, Large number of spikes and irregular structures exists in output DSM. This is mainly because of the poor image matching at the areas with similar textures like roads. The result is worst in case of areas covered by trees and other features with homogenous distribution.

In case of computer vision, accurate 3D points have been generated even in areas with similar textures like roads and fields. As a result very good visual representation can be seen in those areas. Variations in the elevation range for different DSM's is mainly because of the erroneous point interpolated for locations like trees and vegetation. Robust algorithms like dense image matching based on Triangulation used by AP has failed to generate large number of point clouds in areas covered with vegetation and as a result high elevation values aren't generated for these regions. However PIX4D is able to well represent the areas covered with trees and vegetation to some extent.

Regarding the output spatial extent, LPS by default takes the minimum and maximum extent of the 3D points in the overall model before generating the output DSM. While in case of AgiSoft, the output extent was calculated from the extent of the pattern in which the images were taken. PIX4D provides more control over the output DSM that we are going to generate. The output DSM from PIX4D covers only those areas where the overlap exists between the images. As a result, the chances of erroneous calculations beyond such areas are reduced during surface reconstruction.

### 3.4 Accuracy Assessment of DSM

#### 3.4.1 Computation of RMSE

Five GCP's has been used as the reference data during accuracy assessment of DSM. Elevation difference was measured at five different locations in every individual DSM's. Then RMSE was calculated for results from each software. Table 9 shows that the most accurate DSM is obtained from PIX4D in terms of output RMSE.

Table 7: Comparison of Elevation of check points with elevation from DSM generated by different software

| Point No        | Elevation (m) |              |              |               | Elevation Difference (cm) |                    |                    |
|-----------------|---------------|--------------|--------------|---------------|---------------------------|--------------------|--------------------|
|                 | Original (O)  | DSM LPS (a)  | DSM AP (b)   | DSM PIX4D (c) | O-a                       | O-b                | O-c                |
| 2003            | 136.173       | 136.278      | 136.116      | 136.201       | -10.54                    | 5.66               | -2.84              |
| 2004            | 128.362       | 128.392      | 128.422      | 128.375       | -3.04                     | -6.04              | -1.34              |
| 2006            | 132.402       | 132.262      | 132.381      | 132.382       | 13.960                    | 2.06               | 1.96               |
| 2007            | 127.585       | 127.649      | 127.653      | 127.571       | -6.44                     | -6.84              | 1.36               |
| 2010            | 131.953       | 132.052      | 131.941      | 131.962       | -9.94-                    | 1.16               | -0.94              |
| <b>RMSE(cm)</b> |               | <b>9.546</b> | <b>4.917</b> | <b>1.813</b>  | <b>Mean= 8.783</b>        | <b>Mean= 4.348</b> | <b>Mean= 1.688</b> |

Table 7 shows that the DSM from LPS has the least accuracy in term of RMSE and mean error. It shows that the use of classical photogrammetric software like LPS isn't suitable for generating high resolution products from UAV imagery. The outputs from software especially designed for processing digital images is satisfactory. The algorithms which are designed to process images with large distortions and inconsistent image geometry has been able to orient the images with cm level precision and helped in generating very high resolution DSM. The major reasons behind this outcome is the fact that the almost all kinds of image distortions

were adjusted using thousands of accurately extracted tie points, images were georeferenced with a minimum error, and also the algorithms using for image matching were robust ones. This statistical approach can't address the overall accuracy of the entire DSM. The numerical value alone doesn't fit for the entire DSM in this project as the check points used for accuracy assessment aren't well distributed throughout the region.

### 3.4.2 Visual Comparison and analysis of output DSM

In situations when check points aren't enough and well distributed throughout the project area, RMSE alone doesn't ensure that the output DSM is of good quality. Visual analysis was also carried out at some particular locations in order to test the results from different software.

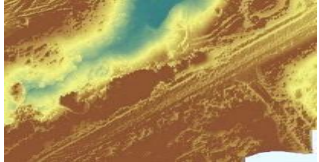
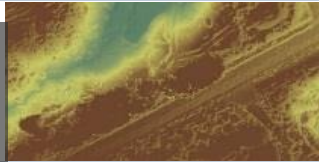
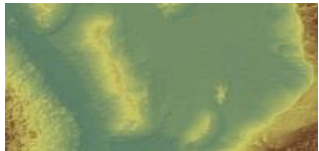
| Actual Image   | Tie Points  | DSM  | Software       |
|--|---|--|----------------|
| <br><i>Surface 1: Areas covered by trees and similar textured Roads</i>                |    |    | AgiSoft Photo- |
|  |   |   |                |
|  |  |  |                |
| <br><i>Surface 2: Heterogeneous area with different objects and terrain structure</i> |  |  | AgiSoft Photo- |
|  |  |  |                |
|  |  |  |                |

Figure 9: Visual Comparison for different Terrain Type

In case of Surface 1, classical photogrammetric software is unable to produce the good results. The number of tie points are also very low and the output DSM has many spikes and irregularities. The use of SIFT algorithm in software like AgiSoft and PIX4D is able to generate large number of tie points in this region. Areas covered with vegetation are still not well represented. This is because of distribution of homogeneous details over a region in case of vegetation. However PIX4D is able to represent such areas to some extent.

Likewise, Surface 2 has been well represented by all the algorithms. Surface 2 contains a combination of different types of objects like artificial objects (vehicles), sand piles and ground with different textures and patterns. As a result the matching has a good result over this region. The output from AgiSoft and PIX4D is able to represent this area in better way. The distribution of accurately matched points in this area as shown in figure 9 is the major reason behind this output.

### 3.4.3 Difference of DSM

Output DSM's from different software were in the format of a raster image. Computations using map algebra helped to calculate the difference between the elevation values of raster SM's at every pixel.

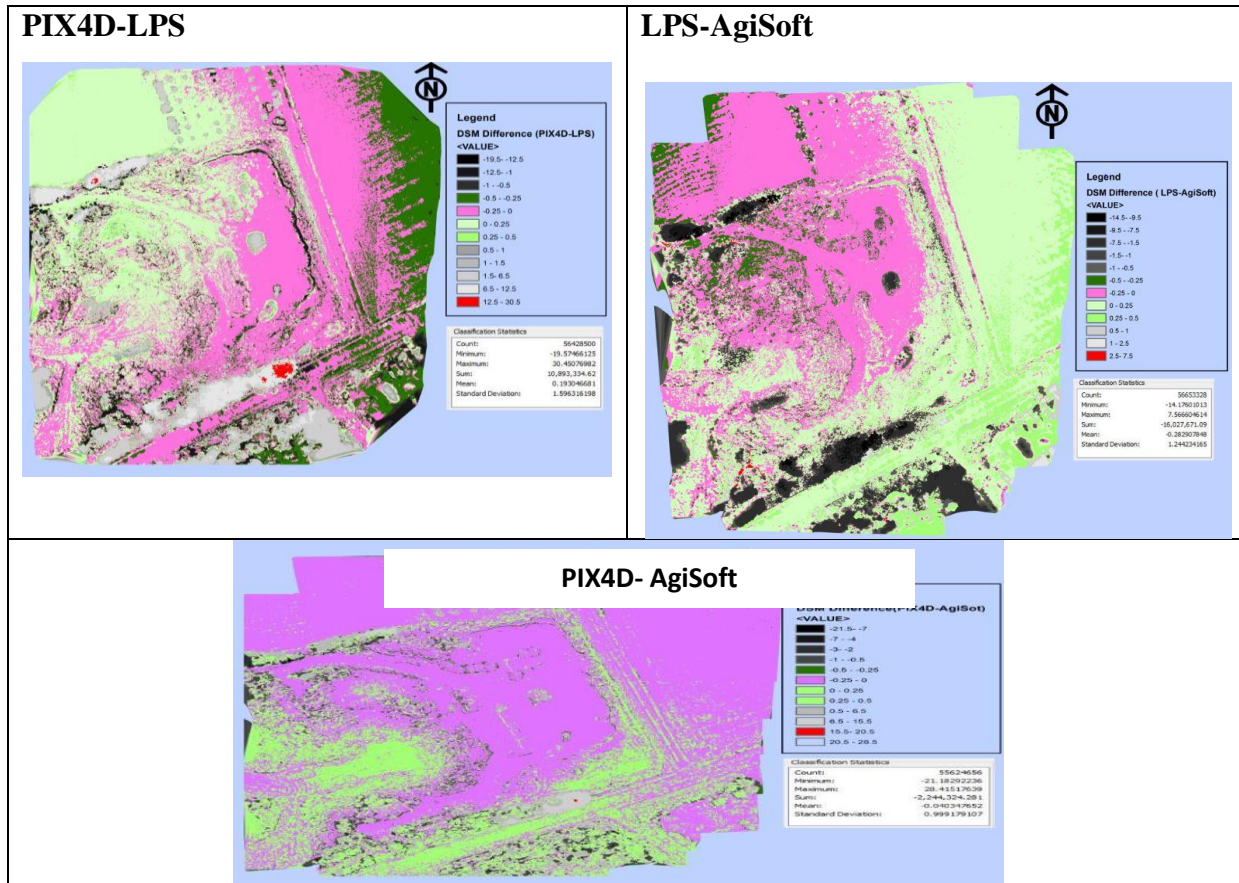


Figure 10: Difference of DSM generated from different Software

## 4. CONCLUSIONS

In this paper we demonstrated the feasibility of generating high resolution digital surface models from digital images captured by a UAV platform. The post processing of UAV-acquired images can be done using algorithms ranging from classical photogrammetry to modern computer vision.

Even though classical photogrammetric image processing software like LPS (version 2011) doesn't have special workflow designed for UAV images, optimization of parameters helped to improve the accuracy of georeferencing and output DSM. Some of such major parameters were introduced in this paper. The computational time is often very high in case of computer vision algorithms. Tie point generation and image matching took some minutes in LPS while in case of AgiSoft Photoscan and PIX4D, feature point extraction took hours for processing. However the greater advantage was that thousands of key points which were extracted in the latter case helped in accurate estimation of image orientation parameters. This further helped for accurate georeferencing of images. The possible cause of errors during georeferencing has been explained.

Automated workflow for DSM generation has been presented in the project. Three DSM's of resolution 0.25 cm were generated from different approaches. Different software use different workflow and they optimize the algorithm in their own way. The comparison shows that algorithms based on computer vision produce better result for georeferencing the images and generating DSM from them. However a lower resolution of the DSM and also inhomogeneous accuracy, over areas covered with trees and vegetation was observed at particular locations in all cases. None of the algorithms were able to create perfect matches for feature points in locations with dense vegetation. As a result its effect was seen in the output DSM where large spikes and irregular surfaces can be seen over such regions.

No algorithms can be optimized perfectly such that they become acceptable for all conditions and applications. Even a very low RMSE cannot solely explain that the output results are satisfactory throughout the region of interest. There are several other reasons behind the variation in the results which are also well explained in respective chapters.

In conclusion, the main objective of the project: to generate high resolution DSM from UAV images is achieved. Both the classical photogrammetric workflows as well as modern techniques based on computer vision were able to give high quality outputs. The RMSE of up-to 8 cm shows that the product from DSM can be used for further applications as well.

## REFERENCES

1. Axelsson, P., *Processing of laser scanner data—algorithms and applications*. ISPRS Journal of Photogrammetry and Remote Sensing, 1999. **54**(2): p. 138-147.
2. Wolf, P.R., B.A. Dewitt, and B.E. Wilkinson, *Elements of Photogrammetry: With Applications in GIS*. Vol. 3. 2000: McGraw-Hill New York.
3. Wang, J., et al., *A New Calibration Model of Camera Lens Distortion*. Pattern Recognition, 2008. **41**(2): p. 607-615.
4. Lee, J.-N. and K.-C. Kwak, *A Trends Analysis of Image Processing in Unmanned Aerial Vehicle*.
5. Van Blyenburgh, P., *UAVs: An Overview*. Air & Space Europe, 1999. **1**(5): p. 43-47.
6. Eisenbeiß, H. and E.T.H. Zürich, *UAV Photogrammetry*. 2009: ETH.
7. Zhang, W. and Y. Wang. *Core Based Structure Matching Algorithm of Fingerprint Verification*. in *16th International Conference on Pattern Recognition, 2002*. 2002. IEEE.
8. Torres, M.Á.A., *Self Calibration Methods for Using Historical Aerial Photographs with Photogrammetric Purposes*.
9. Gini, R., et al., *UAV Photogrammetry: Block Triangulation Comparisons*. ISPRS-International Archives of the Photogrammetry, Remote Sensing and Spatial Information Sciences, 2013. **1**(2): p. 157-162.
10. Luhmann, T. and G. Altrogge, *Interest Operator for Image Matching*. IAPRS-International Archives of Photogrammetry and Remote Sensing, 1986. **26**: p. 3.
11. Jazayeri, I. and C. Fraser, *Interest Operators in Close Range Object Reconstruction*. International Archives of Photogrammetry, Remote Sensing and Spatial Information Sciences, 2008. **47**: p. 69-74.
12. Lingua, A., D. Marenchino, and F. Nex, *Performance Analysis of the SIFT Operator for Automatic Feature Extraction and Matching in Photogrammetric Applications*. 2009. **9**(5): p. 3745-3766.

13. Lowe, D.G., *Distinctive Image Features from Scale-Invariant Keypoints*. International Journal of Computer Vision, 2004. **60**(2): p. 91-110.
14. Schenk, T., *Towards Automatic Aerial Triangulation*. ISPRS Journal of Photogrammetry and Remote Sensing, 1997. **52**(3): p. 110-121.
15. Egels, Y. and M. Kasser, *Digital Photogrammetry*. 2003: CRC Press
16. Zhang, S., et al., *A Dense Stereo Matching Algorithm based on Triangulation*. J. Computer Information System, 2012. **8**(1): p. 283-292.

## **BIOGRAPHICAL NOTES**

The paper is based on the final year Geomatics Engineering 2010 Batch thesis at Kathmandu University.

Email at: [bionicbiplov45@gmail.com](mailto:bionicbiplov45@gmail.com) for any queries or suggestions.

## **CONTACTS**

Title: Biplov Bhandari

Institution: Kathmandu Living Labs

Address: Anamnagar

City: Kathmandu

COUNTRY: NEPAL

Tel. +977-9841926774

Fax +

Email: [bionicbiplov45@gmail.com](mailto:bionicbiplov45@gmail.com)

Web site: <https://www.linkedin.com/pub/biplov-bhandari/72/413/b2b>